



DOI: 10.5137/1019-5149.JTN.12938-14.2

Received: 02.10.2014 / Accepted: 16.12.2014

Original Investigation

Evaluation of Computed Tomography Perfusion Imaging in a Rat Acute Cerebral Ischemia-Reperfusion Model

Xiuhua MA¹, Hua LI², Zhibo XIAO³, Mingquan LI⁴, Peng XUE¹, Yong CHEN¹, Jigang ZHONG¹

¹Zhengzhou People's Hospital, Department of Radiology, Zhengzhou, China

²Rizhao City People's Hospital, Department of Radiology, Rizhao, China

³Chongqing University of Medical Sciences, The First Affiliated Hospital, Department of Radiology, Chongqing, China

⁴Luohe City People's Hospital, Department of Radiology, Luohe, China

ABSTRACT

AIM: This study aims to apply computed tomography perfusion imaging (CTPI) technology under in vivo conditions in order to explore its reliability and accuracy in evaluating the rat acute cerebral ischemia-reperfusion model (RACIRM).

MATERIAL and METHODS: The thread embolism method was used in 48 rats to create the RACIRM. Rats were divided into 2 groups as ischemia group and ischemia-reperfusion group. We then compared and evaluated the results of CTPI, 2,3,5-triphenyl tetrazolium chloride (TTC) staining, and hematoxylin and eosin (HE) staining of both groups.

RESULTS: There were no significant differences in the volumes of hypoperfusion regions in the cerebral blood flow (CBF) and cerebral blood volume (CBV) of each group at each CTPI time point and these volumes were not significantly different from the corresponding findings on the TTC-stained infarct regions. The mean transit time (MTT) did show a significant difference, as did the volumes observed in both the MTT ischemic region and TTC-stained infarct region. The CTPI parameters exhibited correlation with the infarct volumes calculated in TTC staining, among which CBV exhibited the highest correlation.

CONCLUSION: CTPI could rapidly, accurately, and non-invasively evaluate the site, size, and hemodynamic changes in the cerebral ischemia-reperfusion animal model.

KEYWORDS: Computed tomography perfusion imaging, Acute cerebral ischemia, Cerebral hemodynamics, Rat

INTRODUCTION

Acute cerebral ischemia is a common clinical condition with high morbidity and mortality; micro-embolism is one of its important pathogeneses (6,20). Clinically, 85% of cerebral ischemia are caused by occlusion of the middle cerebral artery. In recent in-depth studies on the treatment of acute cerebral ischemia, the acute cerebral ischemia-reperfusion model has been widely used in animal experiments; however, there is still no ideal evaluation method to assess whether the model has been successfully established and to determine the location, extent, and degree of cerebral ischemia, and the post-reperfusion blood flow recovery in the ischemic

regions. Previous studies employed neural scoring to study the acute cerebral ischemia-reperfusion model, but this approach cannot determine either the location or the degree of infarction (14,22). There are recent reports on the use of magnetic resonance imaging (MRI) to evaluate the ischemia reperfusion model (10,15). However, MRI equipment can be expensive to obtain and time-consuming to use, which limits its application. Computed tomography perfusion imaging (CTPI) is a functional imaging method with a simple, convenient, and rapid mode of operation and sophisticated imaging technology, and thus has been gradually applied in various clinical settings. Studies have shown that CTPI can



Corresponding author: Xiuhua MA

E-mail: xiuhuamacn@163.com

identify abnormalities 30 minutes after the cerebral ischemic symptoms occur (4,17). However, reports using CTPI to evaluate acute cerebral ischemia-reperfusion models have been limited. In this study, CTPI technology was applied to perform early, in vivo, dynamic, and accurate monitoring and evaluation of the rat acute cerebral ischemia-reperfusion model (RACIRM), and to provide a quick, simple, and accurate detection method for acute cerebral ischemia.

■ MATERIAL and METHODS

This study was carried out in strict accordance with the recommendations in the Guide for the Care and Use of Laboratory Animals of the National Institutes of Health. The animal use protocol has been reviewed and approved by the Institutional Animal Care and Use Committee (IACUC) of Zhengzhou People's Hospital.

Animals and Grouping

Forty-eight healthy adult female Wistar rats, weighing between 220 g and 250 g, were provided by the Experimental Animal Center, Chongqing Medical University and were randomly divided into an ischemia group (group A) and an ischemia-reperfusion group (group B), with 24 rats in each group. We obtained findings at 6 time points (1, 2, 3, 4, 6, and 8 hours) after ischemia, with 4 rats assigned to each time point. We performed neurological impairment scoring, CT perfusion scanning, and histopathological examination at the corresponding time points, respectively, for the Group A rats. The rats in Group B underwent the 12-hour reperfusion after the above ischemic time points, which was followed by neurological impairment scoring, CT perfusion scanning, and histopathological examination.

Preparation of Thread Embolism and Animal Model

Using a 0.236-mm nylon thread (Beijing Shadong Biotechnology Co., Ltd.) cut to a length of 4.5 cm, we added a little silicone at about 0.5 cm from the tip to form a node with a diameter of about 0.28 mm. The thread was then suspended in a ventilated place for more than 24 hours. Using a pen, we marked the thread at approximately 1.8 ± 0.2 cm down to the tip to control the insertion depth. The thread was then disinfected with alcohol (Chuandong Chemical Co., Ltd., Chongqing, China) and heparin-processed (Shandong Qilu Pharmaceutical Co., Ltd., Jinan, China). Using the improved Longa method (8) on fasting (but not water-restricted), anesthetized (3.5% chloral hydrate at 1 g/100 mg [Shanghai Wulian Chemical Co., Ltd., Shanghai, China]) rats, we established the cerebral ischemia-reperfusion model by the thread-embolism method. During the surgery, the rats were fixed in the supine position while we made a 2-cm midline incision in the neck to isolate and expose the right vagus nerve, common carotid artery (CCA), external carotid artery (ECA), internal carotid artery (ICA), and pterygopalatine artery (PPA). The PPA was isolated without ligation, and the ECA branch arteries (namely the occipital artery and superior thyroid artery) were isolated and cut off. We ligated and cut off the ECA near the CCA bifurcation, and then used a small artery clamp (Ningbo medical needle Co., Ltd., Ningbo, China) to clamp the distal end of the CCA and

ICA. The prepared node thread was placed at the ICA without temporarily tightening the thread. We made a V-shaped incision using ophthalmic scissors (Suzhou 66 Vision Technology Co., Ltd., Suzhou, China) at the CCA bifurcation, and then inserted the thread embolism and unplugged the ICA small artery clip. The thread depth was approximately 1.8 ± 0.2 cm, just reaching the start of the middle cerebral artery in order to block the middle cerebral artery (MCA) blood flow. We then tightened the proximal node and pulled out the CCA small artery clasper. The incision was then sutured with the thread bolt placed outside the incision, which eased reperfusion by allowing us to easily move the thread embolism to the CCA site. All the animals were kept at a body temperature of 25 to 28°C under commercial incandescent lighting during the surgery, and their rectal temperature was maintained at about 37°C, as the ECA and CCA along the vagus nerve should be protected to avoid stimulating the trachea during the artery separation process.

Neurological Impairment Scoring

After the surgery, animal behaviors were observed both immediately following and at the different reperfusion time points in order to perform the neurologic impairment scoring. We used the 5-grade neurologic impairment scoring method established by Longa et al. (8) to evaluate rat nerve damage as follows: 0 points, normal activity, no neurological deficit symptoms; 1 point, the contralateral forelimb could not fully extend; 2 points, legs cycled contralaterally when crawling; 3 points, the body fell towards the hemiplegic side when walking; and 4 points, the animal could not walk spontaneously and lost consciousness.

CTPI and Image Processing

The GE LightSpeed 64-slice CT scanner was used for imaging, with scanning parameters of 80kV tube voltage, 100 mA tube current, a 512 × 512 matrix, and a 9.8 cm field of view. After the rats were anesthetized and fixed in the prone position, we used a 24 G intravenous remaining needle to puncture the tail vein, followed by fixation and connection with a high-pressure syringe. The normal and lateral positioning images were scanned first, after which continuous coronal dynamic perfusion scanning with 2.5-mm-thick slices was performed from the cerebral front pole, using the cine collection method (i.e., one layer(s) with a total of 16 images covering the 40-mm range); thus, the continuous 40-second scanning procedure yielded a total of 640 images. When the perfusion scanning started, we simultaneously injected 2 ml of non-ionic contrast agent Ultravist (370 mg/ml) (Bayer Schering Pharma, Guangzhou, China) with an injection flow rate of 0.2 ml/s.

The perfusion scanning images were input into the ADW 4.2 image workstation, and processed by the Brain Stroke software (CT Perfusion) to generate bilateral cerebral blood flow (CBF), cerebral blood volume (CBV), and mean transit time (MTT) images of different levels. The bilateral symmetric regions of interest (ROIs) of lesion sites in the above functional images were selected and the CBF, CBV, and MTT of each ROI were recorded. The results of CTPI parameter images were then compared with the TTC staining images, and the ROIs were

divided into three groups: (1) the central infarct region showing decreased CBF and CBV and white 2,3,5-triphenyl tetrazolium chloride (TTC) staining; (2) the penumbra region showing decreased CBF, normal or mildly elevated CBV, and pink TTC staining; and (3) the region with relatively normal CBF and CBV and red TTC staining. The areas of the different lesion layers in the CBV central infarct region, CBV hypoperfusion region, and MTT ischemic region were measured and then multiplied by the layer thickness to yield the lesion volume in the images obtained for these three parameters, and these results were then compared with the TTC-stained infarct volumes.

Histopathological Examination

After the CT examination, the rats were decapitated and the samples frozen at -20°C for 20 minutes. Next, based on the layers assessed in CT perfusion scanning, 5 to 6 continuous coronal slices of 1.5 to 2 mm thickness were cut, moving back from 2 mm of the frontal pole. These slices were then placed in a 2% TTC buffer solution (Shanghai Jingtian bio Co., Ltd., Shanghai, China) for 30 min of staining in a dark room at a temperature of 37°C. In this method, when a digital camera was used to photograph (SONY DSC-P200, Japan) these slices, the normal tissues would appear red, the infarct tissues would appear white, and the ischemic areas would thus appear pink. The photographs were then entered into a computerized pathological image analysis system to measure the infarct area of each layer and calculate the infarct volume. The TTC-stained slices were then dehydrated and decolorized with ethanol, fixed in 10% paraformaldehyde (Chengdu Kelong Chemical Reagent Factory, Chengdu, China), dehydrated, hyalinized, paraffin-embedded, and sliced for the hematoxylin and eosin (HE) staining.

Statistical Analysis

All the data were expressed as “x±s”, and the SPSS 10.0 statistical software was used to calculate both analysis of variance and linear correlation analysis, with p < 0.05 considered to indicate significant differences.

RESULTS

In group A, 2 rats died at the post-ischemic 4- and 8-hour time points, respectively. In group B, 5 rats died of brain

hemorrhage at the post-ischemic 1-, 2-, 3-, 4-, and 8-hour time points, respectively; thus, a total of 7 rats were excluded from the statistical analysis.

Neurological Impairment

While all the rats exhibited neurological deficit symptoms post-surgery, and scored between 1 and 4 points on the Longa-created scale, there was no significant difference in these scores 1 hour after ischemia (p > 0.05), indicating that the conditions of cerebral ischemia were consistent. The deficit symptoms of the ischemia group and the reperfusion group did not change significantly over time, and there was no statistically significant difference in the scores (p > 0.05). Only the intergroup comparison of neurological deficit symptoms revealed a statistically significant difference (p < 0.05) (Figure 1).

Changes and Relationships of CTP-Parameter Images and TTC

The TTC staining results in each group revealed no contralateral infarct lesions, while the infarct volume of the ischemic side extended over time. Although the infarct volumes at the 1- and 2-hour time points showed significant differences when compared with those at the 3-, 4-, 6-, and 8-hour time points (p < 0.05), there was no significant difference between the 1- and 2-hour (p > 0.05) time points and no statistically significant difference at the 3-, 4-, 6-, and 8-hour (p > 0.05) time points. There was also no statistically significant difference in the volumes of CBF core area (Figure 2A) and CBV low-perfusion area (Figure 2B) at each CTPI time point (p > 0.05). The volumes exhibited by both showed no significant difference with that of the TTC staining infarct region (Figure 2D, p > 0.05), although they did show a statistically significant difference with the volume of the MTT ischemic region (Figure 2C, 2D; p < 0.05). The volume of the TTC staining infarct region showed a significant difference with that of the MTT ischemic region (p < 0.05). Finally, the CTP parameter images exhibited correlations with TTC staining infarct volumes, among which the CBV correlation was the highest (Table I, II).

Changes and Relationships of CTPI Parameters and HE Staining

Because the ischemic time was different, the cerebral tissues

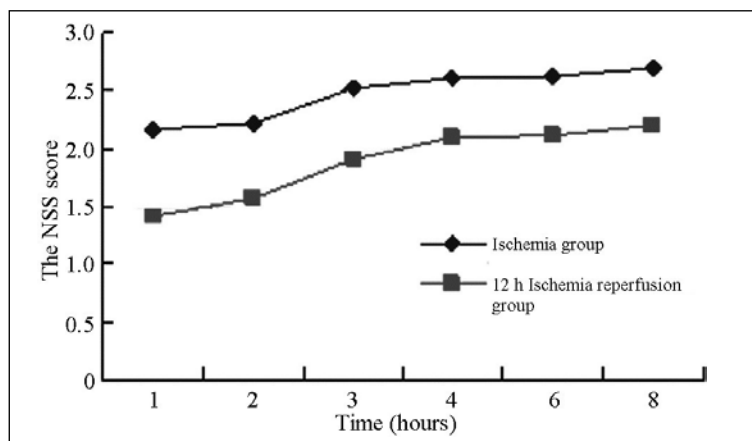


Figure 1: NSS scores of the group A and B at the different time points had the significant differences, p < 0.05.

exhibited clear differences in CTPI and HE staining. In group A, ischemic cerebral edges exhibited reduced CBF in the ischemic 1-, 2-, and 3-hour subgroups, while CBV was normal, reduced, or increased, and MTT was prolonged. Light microscopy after HE staining revealed widened vascular gaps, a reduction in the number of neurons, edema in the nerve cell, and partial nerve karyopyknosis. In group B, CBF was reduced or normal, while CBV was normal or increased, and the HE staining indicated slightly heavier swelling than that seen in group A. The ischemic 4-, 6-, and 8-hour subgroups showed that CBF and CBV in the ischemic area were reduced (Figures 2A, 2B), while MTT was extended (Figure 2C). The HE staining showed significantly widened neuronal gaps, nerve karyopyknosis, and significant nerve cell edema. Further, the neuronal distortion or shrinkage was obvious, most of the nerve terminals appeared vacuolar, the organelles disappeared, and the inner structure of myelin sheath dissolved (Figure 3A, B).

DISCUSSION

The use of RACIRM required extensive preparation, including cranial mechanical occlusion, and the photochemistry-induced thrombosis, suture-embolism, and microemboli embolism methods. This study used the improved Longa suture-embolism method (8, 13, 22, 23), which offered advantages such as no need of craniotomy, less damage, simplicity of operation, relatively consistent location of the ischemic area, and accurate control of ischemia and reperfusion time, and thus could facilitate the study of reperfusion injuries and the selection of treatment window. It is a popular model preparation method around the world, and it is especially suitable for research involving ischemia reperfusion models (1,9). In this study, the RACIRM was successfully established using the embolism method, without ligation of the PPA, and therefore reduced both the chance of thrombosis and the surgical time. Post-surgery, the neurological deficit scores of the rats were between 2 and 3 points, indicating good embolism effects, and the scores before and after the perfusion showed significant differences. Their observed behavior reflected the success of implementing ischemia reperfusion by the embolism method. The post-neurological scores and mortalities in group B (the

reperfusion group) were also higher than those in group A (the ischemia group), indicating that reperfusion represented a secondary injury to acute cerebral ischemia.

Since the theoretical basis of CTPI was the radiotracer dilution principle and the central volume laws of nuclear medicine, during the intravenous injection of contrast agent, the selected layers were exposed to continuous multiple scanning in order to obtain the “time–density” curve of each pixel within this layer. This curve was then used to calculate the perfusion parameters by different mathematical models, so that the states of tissue and organ perfusion could be evaluated (16,18). Since CPTI was capable of identifying the ischemic lesions and determining their scope and extent in hyperacute cerebral infarction even before the ischemic tissues exhibited morphological changes, it can be considered as a functional imaging examination method (2, 3). Our study used 64-slice spiral CT, which overcame the shortcomings of range limits in previous single- and multi-slice spiral CT perfusion scanning. Further, the scanning layers employed by this method included the rats’ entire brain and partial neck, and the method allowed faster scanning, higher time and spatial resolution, and the use of more accurate and feature-rich post-processing software. The CTPI parameter images obtained at the different time points could dynamically reflect the blood flow changes in hyperacute cerebral ischemia, and CBF, in particular, exhibited high sensitivity and specificity for cerebral ischemia determination. In addition, CTPI can display the cerebral ischemic volume, and the CBF and the CBV images showed no significant difference in ischemic volume measurement. While CTPI did exhibit a significant difference with MTT, the MTT image showed a larger ischemic volume, indicating that MTT would be more sensitive than the other parameters for early identification of ischemic lesions. This result was consistent with Nabavi’s findings (5, 12, 21). The ischemic volumes in the CBF and CBV parameter images showed no significant difference with the TTC staining results. While the MTT ischemic volume exhibited significant differences with the TTC staining results, these 3 images were correlated with the TTC staining infarct volumes, indicating that while the CBV’s association was better, MTT and CBF would often overestimate the infarct volumes, which was related to the

Table 1: Ischemic Region volumes by TTC and CTPI Parameter Images After Middle Cerebral Artery Occlusion (MCAO) and 12h After the Reperfusion (mm³, $\bar{x} \pm s$)

Ischemic time	Group A				Group B			
	TTC	CBV	CBF	MTT	TTC*	CBV*	CBF*	MTT*
1h	81.75±44.01	89.23±32.56	101.23±45.25	117.21±42.36'	31.75±9.35	34.52±11.21	41.25±21.14	49.54±35.28'
2h	87.54±52.65	94.57±25.68	114.82±36.87	134.36±45.25'	39.24±8.96	42.36±25.21	47.52±31.57	54.21±35.25'
3h	122.37±29.36	143.56±36.57	153.58±63.14	178.52±35.18'	101.25±24.75	115.65±32.29	134.53±54.21	156.36±26.85'
4h	137.47±34.54	157.56±63.13	175.54±36.24	198.35±52.23'	112.63±63.25	135.65±35.63	152.43±37.85	182.12±42.19'
6h	142.56±52.47	169.53±35.89	196.32±65.41	214.63±39.85'	129.36±36.53	145.63±63.52	178.69±65.14	213.25±39.85'
8h	156.98±43.58	168.32±63.21	189.65±39.54	206.38±52.13'	152.63±63.21	161.21±32.36	179.89±36.85	190.58±42.19'

'p < 0.05 compared with TTC in each group; *p < 0.05 compared with Group B.

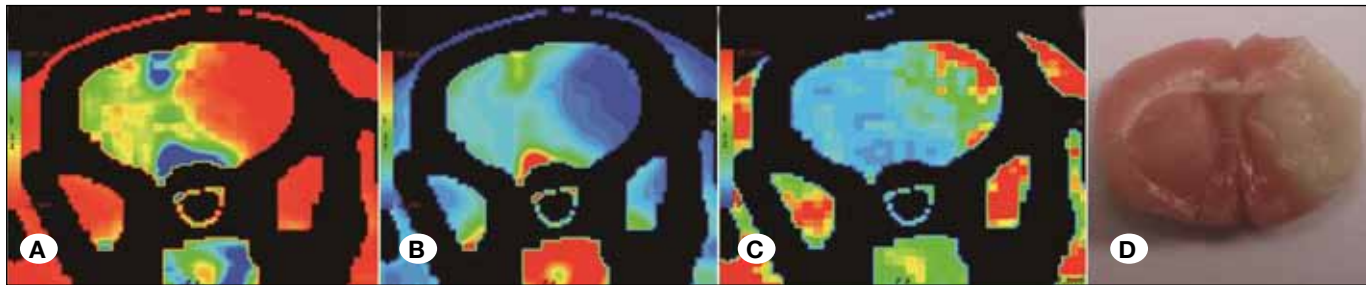


Figure 2: Comparison of infarct ranges of middle cerebral artery occlusion (MCAO) 8h, CTPI parameter images and MTT staining-exhibited right cortex and basal ganglia. **A)** CBF figure, which was significantly reduced in the right red zone, namely the infarction region; **B)** CBV figure, which was significantly reduced in the right blue area, namely the infarction region; **C)** MTT figure, the green and red areas were the MTT extension, namely the infarction region; **D)** MTT staining figure, the right white region was the infarction range.

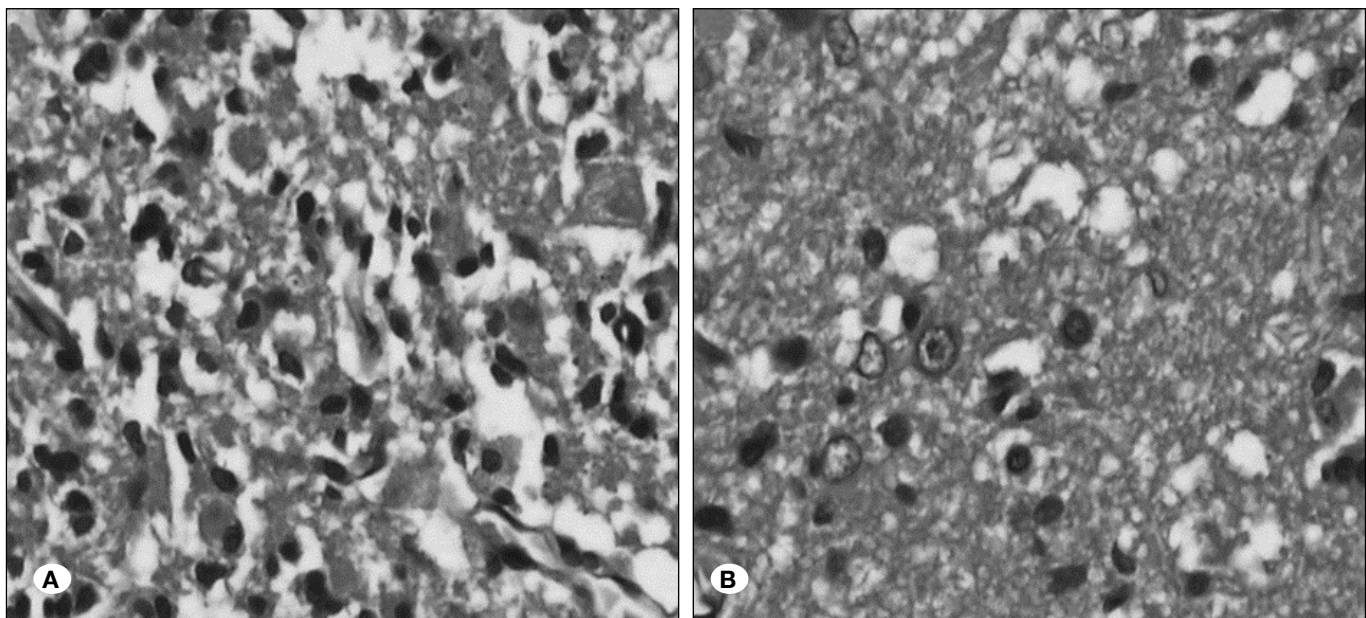


Figure 3: Changes of cortical ischemic tissues in middle cerebral artery occlusion (MCAO) 6h and 12h after the reperfusion, the nerve cells were lost to the various degrees (HE staining $\times 400$). **A)** MCAO 6h; **B)** MCAO 6h-reperfusion 12h, the neuronal gaps in the cortical ischemic region were significantly widened, the nerve karyopyknosis appeared, and the edema of nerve cells was obvious. Most nerve terminals showed vacuolization, the organelles disappeared, and the structures inside the myelin sheath were dissolved (HE staining $\times 400$).

Table II: Correlation Analysis of CTPI Parameter Images and TTC Staining Ischemic Volumes

Result	CBV	CBF	MTT
Pearson coefficient	0.74	0.52	0.41
P	<0.05	<0.05	<0.05

The CTPI parameter images were correlated with the TTC staining infarct volumes.

sensitivity of MTT and CBF in showing ischemia. The CTPI signals towards the lesion central area, marginal region, and relatively normal tissue regions were significantly different, exhibiting low to high ladder-like changes, and corresponding to the pale infarct area, pink ischemic area, and red normal

tissue area in the TTC staining; thus, CTPI could exhibit the semi-penumbra with higher sensitivity and specificity towards the cerebral ischemia. These findings are basically consistent with previous studies (5, 7, 12, 19, 21). Nabavi et al. (12) found that the sensitivities of TTP, CBF, and CBV in diagnosing cerebral ischemia were 72.6%, 64%, and 58.9%, respectively. Murphy et al. (11) found that the sensitivity of the CBF-CBV combination in diagnosing cerebral ischemia was 90.6%, with a specificity of 93.3%. In our study, all of our statistical models of the infarct region showed that CBF and CBV were reduced and MTT was prolonged, CBF in the ischemic area was reduced and MTT was extended, while CBV either displayed no significant changes or mildly increased or decreased. The non-matching of CBV and CBF was related to the self-regulation mechanism of acute cerebral ischemia, and it was also a characteristic change of cerebral ischemic semi-penumbra. These results were consistent with the HE staining.

Currently, the main evaluation methods for the cerebral ischemia-reperfusion model include neurological impairment symptom scoring, laser Doppler measurements of the changes in cerebral blood flow, MRI (diffusion-weighted imaging and perfusion-weighted imaging), TTC staining, and HE staining. The first two offered greater subjectivity, but lacked effective quantitative criteria, and the latter two could not achieve evaluation in the *in vivo* state. That leaves functional imaging techniques such as MRI and CT as the best options, although MRI has a longer history and thus is considered the preferred technique despite the expense and the length of time required for imaging. Although CTPI has not been in use as long as the MRI as a functional imaging technique, its simple and convenient operation and high spatial resolution, sensitivity, accuracy, and repeatability makes it an attractive alternative. Our study showed that in acute cerebral ischemia, CTPI could accurately reflect the situations of ischemia and reperfusion, non-invasively evaluate the changes of cerebral hemodynamics, and exhibit the infarct and ischemic locations, sizes, and extents, thereby representing a more effective, efficient, practical, and intuitive evaluation method for the cerebral ischemia-reperfusion model. Most importantly, CTPI examination was fast, the normal scanning, perfusion scanning, and image processing could be finished within a few minutes, which would greatly reduce the clinical treatment window, and thus offer a strong basis for clinical treatment and review, especially for hyperacute cerebral infarction. However, CTPI also has issues that need to be resolved, such as the subjective measurement of infarct volume, X-ray radiation dose exposure, animal tolerance to the contrast agents, and the impact of anesthetics on cerebral oxygen metabolism and blood flow. More studies are necessary to examine these factors and their effects.

■ REFERENCES

- Doerfler A, Schwab S, Hoffmann TT, Engelhorn T, Forsting M: Combination of decompressive craniectomy and mild hypothermia ameliorates infarction volume after permanent focal ischemia in rats. *Stroke* 32: 2675-2681, 2001
- Ginsberg MD: Neuroprotection for ischemic stroke: Past, present and future. *Neuropharmacology* 55: 363-389, 2008
- Hetze S, Römer C, Teufelhart C, Meisel A, Engel O: Gait analysis as a method for assessing neurological outcome in a mouse model of stroke. *Neurosci Methods* 206: 7-14, 2012
- Hu L, Gao PY: Study of swelling of local cerebral astrocytes with CT perfusion and histopathological technique in rats. *Chinese CT MRI* 1: 20-22, 2003
- Jauch EC, Saver JL, Adams HP Jr, Bruno A, Connors JJ, Demaerschalk BM, Khatri P, McMullan PW Jr, Qureshi AI, Rosenfield K, Scott PA, Summers DR, Wang DZ, Wintermark M, Yonas H: Guidelines for the early management of patients with acute ischemic stroke a guideline for healthcare professionals from the American Heart Association. American Stroke Association. *Stroke* 44: 870-947, 2013
- Koch S, Amir M, Rabinstein AA, Reyes-Iglesias Y, Romano JG, Forteza A: Diffusion-weighted magnetic resonance imaging in symptomatic vertebrobasilar atherosclerosis and dissection. *Arch Neurol* 62: 1228-1231, 2005
- Liu J, Wang Y, Yang Y, Jiang X, Wu G, Wu J, Zheng M, Peng S: Pyrolo[1,2:4,5] -1,4-dioxopyrazino[1,2:1,6] -pyrido [3,4-b] indoles: a group of urokinase inhibitors, their synthesis and stereochemistry -dependent activity. *Chem Med Chem* 6: 2312-2322, 2011
- Longa EZ, Weinstein PR, Carlson S, Cummins R: Reversible middle cerebral artery occlusion without craniotomy in rat. *Stroke* 20: 84-91, 1989
- Mei S, Liu J, Zhao M, Wang W, Wang Y, Wu G, Zheng M, Peng S: From Cerius based stereoview to mouse and enzyme: The model systems for discovery of novel urokinase inhibitors. *Mol Biosyst* 7: 2664-2669, 2011
- Melhem ER, Mori S, Mukundan G, Kraut MA, Pomper MG, van Zijl PC: Diffusion tensor MR imaging of the brain and white matter tractography. *AJR Am J Roentgenol* 178: 3-16, 2002
- Murphy BD, Chen X, Lee TY: Serial changes in CT cerebral blood volume and flow after 4 hours of middle cerebral occlusion in an animal model of embolic ischemia. *AJNR* 28: 743-749, 2007
- Nabavi DG, Cenic A, Henderson S, Gelb AW, Lee TY: Perfusion mapping using computed tomography allows accurate prediction of cerebral infarction in experimental brain ischemia. *Stroke* 32: 175-183, 2001
- Nabavi DG, Dittrich R, Kloska SP, Nam EM, Klotz E, Heindel W, Ringelstein EB: Window narrowing: A new method for standardized assessment of the tissue at risk-maximum of infarction in CT based brain perfusion maps. *Neurol Res* 29: 296-303, 2007
- Schaar KL, Breneman MM, Savitz SI: Functional assessments in the rodent stroke model. *Exp Transl Stroke Med* 2: 13, 2010
- Sotak CH: The role of diffusion tensor imaging in the evaluation of ischemic brain injury-a review. *NMR Biomed* 15: 561-569, 2002
- Taguchi A, Kasahara Y, Nakagomi T, Stern DM, Fukunaga M, Ishikawa M, Matsuyama T: A reproducible and simple model of permanent cerebral ischemia in CB-1 7 and SCID mice. *J Exp Stroke Transl Med* 3: 28-33, 2010
- Tomandl BF, Klotz E, Handschu R, Stemper B, Reinhardt F, Huk WJ, Eberhardt KE, Fateh-Moghadam S: Comprehensive imaging of ischemic stroke with multisection CT. *Radiographics* 23: 565-592, 2003
- Wakabayashi K, Nagai A, Sheikh AM, Shiota Y, Narantuya D, Watanabe T, Masuda J, Kobayashi S, Kim SU, Yamaguchi S: Transplantation of human mesenchymal stem cells promotes functional improvement and increased expression of neurotrophic factors in a rat focal cerebral ischemia model. *Neurosci Res* 88: 1017-1025, 2010
- Wan D, Zhu HF, Luo Y, Xie P: Changes in synapse quantity and growth associated protein 43 expression in the motor cortex of focal cerebral ischemic rats following Catalpol treatment. *Neur Regeneration Research* 6: 1380-1386, 2011
- Wang X, Lam WW, Fan YH, Graham CA, Rainer TH, Wong KS: Topographic patterns of small subcortical infarcts associated with MCA stenosis: A diffusion-weighted MRI study. *J Neuroimaging* 16: 266-271, 2006

21. Yang G, Zhu H, Zhao M, Wu J, Wang Y, Wang Y, Zheng M, Chen M, Liu J, Peng S: The application of tetrahydroisoquinoline-3-carbonyl-TARGD (F) F as anti-thrombotic agent having dual mechanisms of action. *Mol Biosyst* 8: 2672-2679, 2012
22. Zhao J, Li G, Zhang Y, Su X, Hang C: The potential role of JAK2/STAT3 pathway on the anti-apoptotic effect of recombinant human erythropoietin (rhEPO) after experimental traumatic brain injury of rats. *Cytokine* 56: 343-350, 2011
23. Zhu HF, Wan D, Luo Y, Zhou JL, Chen L, Xu XY: Catalpol increases brain angiogenesis and Up-Regulates VEGF and EPO in the rat after permanent middle cerebral artery Occlusion. *Int J Bio1 Sci* 6: 443-453, 2010